# Chapter 2
# Colour Measurements and Modeling

**Shyam N. Jha**

The most common property to measure quality of any material is its appearance. Appearance includes colour, shape, size and surface conditions. The analysis of colour is especially an important consideration when determining the efficacy of variety of postharvest treatments. Consumers can easily be influenced by preconceived ideas of how a particular fruit or vegetable or a processed food should appear, and marketers often attempt to improve upon what nature has painted. Recently colour measurements have also been used as quality parameters and indicator of some inner constituents of the material. In spite of the significance of colour in food industries, many continue to analyze it inadequately. This chapter deals with theory of colour, colour scales and its measurement, sampling techniques, and modeling of colour values for correlating them with some internal quality parameters of selected fruits.

## 2.1 Light and Colour

Among the properties widely used for analytical evaluation of materials, colour is unique in several aspects. While every material can be said to possess a specific property such as mass, no material is actually coloured as such. Colour is primarily an appearance property attributed to the spectral distribution of light and, in a way, is related to (source of radiant energy) the illuminant the object to which the colour is ascribed, and the eye of the observer. Without light or the illuminant, colour does not exist. Therefore, several factors that influence the radiation subsequently affect the exact colour that an individual perceives. Those factors are:

- spectral energy distribution of light,
- conditions under which the colour is viewed,
- spectral characteristics of the object with respect to absorption, reflection, and transmission, and
- sensitivity of the eye.

S.N. Jha (✉)
Central Institute of Post-Harvest Engineering and Technology, Ludhiana 141004, Punjab, India
e-mail: snjha_ciphet@yahoo.co.in

S.N. Jha (ed.), *Nondestructive Evaluation of Food Quality*,
DOI 10.1007/978-3-642-15796-7_2, 

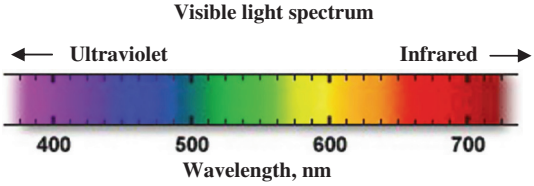


**Fig. 2.1** Colour spectra of light in visible range of wavelength

Light is the basic stimulus of colours, it is important to consider the electromagnetic spectrum. Visible light forms only a small part of the electromagnetic spectrum, with a spectral range from approximately 390 nm (violet) to 750 nm (red) (Fig. 2.1). Wavelength intervals of major colour are summarized in Table 2.1. The sensitivity of the eye varies even within this narrow visible range. Under conditions of moderate-to-strong illumination, the eye is most sensitive to yellow-green light of about 550 nm (Fig. 2.2).

If the spectral distribution throughout the visible region is unequal, then the sensation of colour is evoked by radiant energy reaching the eye's retina. An equal spectral distribution makes the light appear as white. The unequal distribution responsible for colour sensation may be characteristic of the source itself; such as flame spectra (Fig. 2.2) composed of one or more monochromatic wavelengths, or may result from selective absorption by the system, which appears coloured. The latter includes several systems that show selective absorption for light and exhibit colour as a result of reflection or transmission of unabsorbed incident radiant energy. The radiant energy emitted by the radiator is characterized by its spectral quality, angular distribution, and intensity.

The following material properties, lighting of the scene and interaction of matter with light affect the total appearance of the object:

(i) Material properties:

Optical properties (spectral, reflectance, transmittance)
Physical form (shape, size, surface texture)
Temporal aspects (movement, gesture, rhythm)

**Table 2.1** Breakup of wavelengths for major colours in visible range of wavelength

| Colour | Wavelength interval | Frequency interval |
|---|---|---|
| Red | ~ 700–635 nm | ~ 430–480 THz |
| Orange | ~ 635–590 nm | ~ 480–510 THz |
| Yellow | ~ 590–560 nm | ~ 510–540 THz |
| Green | ~ 560–490 nm | ~ 540–610 THz |
| Blue | ~ 490–450 nm | ~ 610–670 THz |
| Violet | ~ 450–400 nm | ~ 670–750 THz |

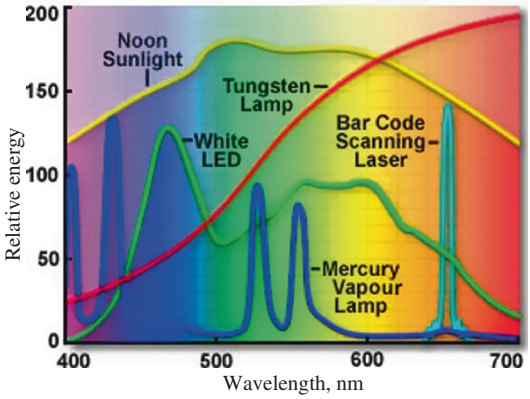


**Fig. 2.2** Spectra of visible light from common light sources

(ii) Lighting of the scene:

Illumination type (primary, secondary, tertiary)
Spectral and intensity properties; directions and distributions
Colour-rendering properties

(iii) Interaction of light with matter

(a) Physical laws

When light falls on an object, it may be reflected, transmitted, or absorbed (Fig. 2.3). Reflected light is the part of the incident energy that is bounced off the object surface, transmitted light passes through the object, and absorbed light constitutes the part of the incident radiant energy absorbed within the material. The degree to which these phenomena take place depends on the nature of the material and on the particular wavelength of the electromagnetic spectrum being used. Commonly, optical properties of a material can be defined by the relative magnitudes of reflected, transmitted, and absorbed energy at each wavelength. Conservation of energy requires that sum of the reflected ($I_R$), transmitted ($I_T$), and absorbed ($I_A$) radiation equals the total incident radiation ($I$). Thus,

$$I = I_R + I_T + I_A \tag{2.1}$$

According to its transmittance properties, an object may be transparent, opaque, or translucent. Almost all food and biological products may be considered to be opaque, although most transmit light to some extent at certain wavelengths. The direction of a transmitted ray after meeting a plane interface between any two non-absorbing media can be predicted based on Snell's law:

$$n_2 \sin \theta_T = n_1 \sin \theta_i \tag{2.2}$$

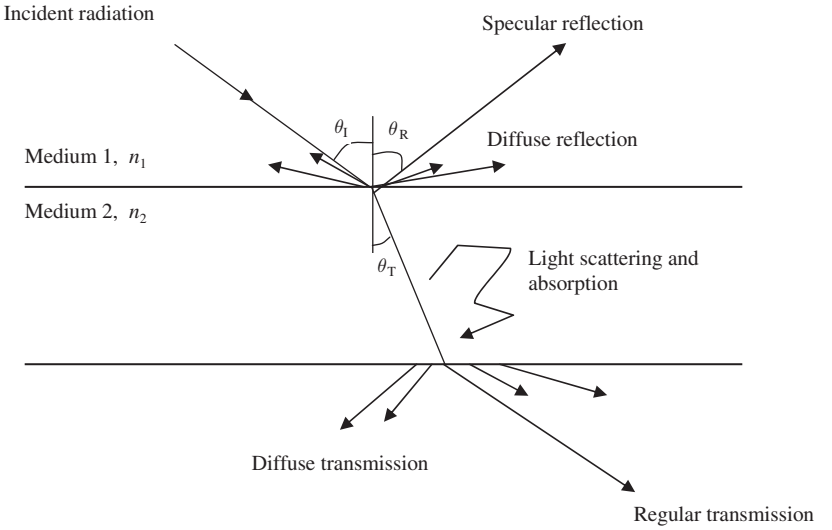


**Fig. 2.3** Schematic representation of interaction of light with matter, $\theta_I$= angle of incidence, $\theta_R$ = angle of reflectance, $\theta_T$ = angle of transmittance, $n_1$, $n_2$ = refractive index of medium 1 and 2, respectively

Beer-Lambert's law defines the attenuation of the transmitted ray in a homogeneous, non-diffusing, absorbing medium:

$$\log\ (I_T/I) = abc \tag{2.3}$$

The ratio $I_T/I$ is known as the transmittance $T$ and is related to absorbance $A$ as:

$$A = \log(I/T) \tag{2.4}$$

From Eqs. (2.3) and (2.4), absorbance $A$ can also be written as:

$$A = abc \tag{2.5}$$

where $a$ is called the absorptivity. [if $c$ is expressed in *mol/L* and $b$ in *cm*, $a$ is replaced by the molar absorptivity, $\varepsilon$ (*L/mol.cm*).]

Various constituents of food products can absorb a certain amount of this radiation. Absorption varies with the constituents, wavelength, and path length of the light. Reflection is a complex action involving several physical phenomena. Depending on how light is reflected back after striking an object, reflection may be defined as regular or specular and diffused (Fig. 2.3). Reflection from a smooth, polished surface is called" specular" or "regular". It mainly produces the gloss or shine of the material. The basic law of specular reflection states that the angle at which a ray is incident to a surface must equal the angle at which it is reflected off the surface. Fresnel equations define the phenomenon of specular

reflection. The intensity of parallel $R_{pl}$ and perpendicular $R_{pr}$ components of the reflected light are:

$$R_{pl} = \left[ \frac{(n_2/n_1)^2 \cos\theta_I - [(n_2/n_1)^2 - \sin^2\theta_I]^{1/2}}{(n_2/n_1)^2 \cos\theta_I + [(n_2/n_1)^2 - \sin^2\theta_I]^{1/2}} \right]^2 \tag{2.6}$$

$$R_{pr} = \left[ \frac{\cos\theta_I - [(n_2/n_1)^2 - \sin_2\theta_I]^{1/2}}{\cos\theta_I + [(n_2/n_1)^2 - \sin^2\theta_I]^{1/2}} \right]^2 \tag{2.7}$$

The regular reflectance $R = R_{pl}{}^2 + R_{pr}{}^2$ and for normal incidence ($\theta = 0°$), $R_{pl} = R_{pr,}$ and hence.

$$R = \left[ \frac{n_2 - n_1}{n_2 + n_1} \right]^2 \tag{2.8}$$

where $n_1$ and $n_2$ are refractive index of the medium and object, respectively: and $\theta_I$ is the incident angle (Fig. 2.3). If the material is absorbing, the refractive index is a complex number $n$ (1-$ik$), where $n$ is the real part of the complex number and $k$ is an absorption constant, and the regular reflectance is written as:

$$R = \left[ \frac{(n_2 - n_1)^2 + (n_2 k)^2}{(n_2 + n_1)^2 + (n_2 k)^2} \right] \tag{2.9}$$

When the incident light is reflected from a surface evenly at all angles, the object appears to have a flat or dull finish termed "diffuse reflection". No rigorous theory has been developed for diffuse reflectance, but several phenomenological theories have been proposed, the most popular being the Kubelka-Munk theory. The Kubelka-Munk model relates sample concentration to the intensity of the measured spectrum in a manner analogous to the way Beer-Lambert's law relates band intensities to concentration for transmission measurements. The Kubelka-Munk function $f(R_\infty)$ is generally expressed as:

$$f(R_\infty) = \frac{(1 - R_\infty)^2}{2R_\infty} = \frac{k}{s} \tag{2.10}$$

where $R_\infty$ = absolute reflectance of an infinitely thick layer, $k$ = absorption coefficient, and s = scattering coefficient.

Kubelka-Munk theory predicts a linear relationship between spectral data and sample concentration under conditions of constant scattering coefficient and infinite sample dilution in a non-absorbing matrix such as KBr (potassium bromide). Hence, the relationship can only be applied to highly diluted samples in a non-absorbing matrix. In addition, the scattering coefficient is a function of particle size, so samples must be prepared to a uniform fine size for quantitative valid measurements.

It is not easy to quantify diffuse reflectance measurements since sample transmission, scattering, absorption, and reflection all contribute to the overall effect. By reducing particle size and dilution in appropriate matrices, surface reflection that can give strong inverted bands is reduced and the spectra more closely resemble transmission measurements. Typically, quantitative diffuse reflectance measurements are presented in log(*I*/*R*) units, analogous to absorbance log(*I*/*T*) units for transmission measurements. Bands increase logarithmically with changes in the reflectance values. By comparison, bands in spectra displayed in Kubelka-Munk units vary as a function of the square of reflectance. This difference emphasizes strong absorbance bands relative to weaker bands.

The diffuse reflectance may be measured with respect to non-absorbing standards and converted to produce a linear relationship with concentration $c$ as follows:

$$\log (R'/R) = \log (I/R) + \log (R') \cong ac/s \tag{2.11}$$

where $R'$ and $R$ – reflectance of the standard and the sample ($R' > R$), $a$ = absorptivity, $c$ = concentration, and $s$ = scattering coefficient. For monochromatic radiation, *log* $R'$ is constant and may be ignored, and Eq. (2.11) may be written as (2.12):

$$c = k + (s/a) \log (I/R) \tag{2.12}$$

where $k$ = absorption coefficient. It should be noted that $s$ is not a constant but depends on a number of properties of the sample such as particle size ($s$ is inversely proportional to particle size) and moisture content. In food materials, the primary factors that influence light reflection is a phenomenon known as scattering or diffusion. If the surface of incidence is rough, incident light will be scattered in all directions. Since the incident rays strike a rough surface more than once before being reflected, they would be expected to have a lower total reflectance than those reflected from a smooth surface.

In classical optics, diffuse reflection was thought to be responsible for colour. It was also commonly believed that colour of natural objects, such as foods, plants and foliage, are seen by means of light reflected off their surfaces. It is also known that the light must be transmitted through pigment within the cells in order to produce a coloured appearance. Since most food materials are optically non-homogeneous, light entering such material is scattered in all directions. Only about 4–5% of the incident radiation is reflected off the surface of these materials as regular reflectance. The remaining radiation transmits through the surface and encounters small interfaces from within the material and is scattered back to the surface through the initial interface. This type of reflection is termed as “body reflectance”. The body reflectance is nearly always diffuse and is the most significant form of reflectance for foods. Some part of the transmitted light diffuse deeper in to the material and may eventually reach the surface some distance away from the incident point.

(b) Factors affecting diffuse reflectance spectral data

Diffuse reflectance spectroscopy offers exceptional versatility in sample analysis. This versatility results from both its sensitivity and optical characteristics. Classically, diffuse reflectance has been used to analyze powered solids in a non-absorbing matrix of an alkali halide such as KBr. The sample is typically analysed at low concentrations, permitting quantitative presentation of the data in Kubelka-Munk unit. This technique yields spectra that are qualitatively similar to those produced by conventional transmittance or pellet methods. However, they exhibit higher sensitivity for quantification and are less subject to scattering effects, that cause slopping baselines in pellet measurements.

Several factors determine band shape and relative/absolute intensity in diffuse reflectance spectroscopy through their effect on the reflection/absorbance phenomena specific to the sample. These include:

refractive index of the sample,
particle size,
sample homogeneity, and
concentration.

*Refractive index*: Refractive index affects the results via specular reflectance contributions to diffuse reflectance spectra. With organic samples, the spectra display pronounced changes in band shape and relative peak intensities, resulting in non-linearity in the relationship between band intensity and sample concentration. For some inorganic samples, strong specular reflection contributions can even result in complete band inversions. Sample dilution in non-absorbing matrix can minimize this overlay of diffuse reflectance and specular reflectance spectra, as well as the resulting spectral distortions. In addition, accessory design can help reduce specular reflectance contributions.

*Particle size*: Particle size is a major consideration when performing diffuse reflectance measurements of solids. The bandwidth is decreased and relative intensities are dramatically altered as particle size decreases. These effects are even more pronounced in spectra of highly absorbing inorganic materials with high refractive indices. For these samples, specular contributions can dominate the final spectra if the particle size is too large. To acquire a true diffuse reflectance spectrum, it is necessary to uniformly grind the sample and dilute it in a fine, non-absorbing matrix. Similar preparation must be applied to the non-absorbing matrix material in order to provide an "ideal" diffuse reflector for background analysis and as a support matrix for the samples.

*Sample homogeneity*: The Kubelka-Munk model for diffuse reflectance is derived for a homogeneous sample of infinite thickness. However, some sample analysis methods, especially those designed for liquid sample (e.g., deposition of sample onto a powdered supporting matrix) can result in a higher concentration of sample near the analysis surface. In these circumstances, variations in relative peak intensities may be noticed. In particular, more weakly absorbing wavelengths tend to be attenuated at higher sample concentrations. To avoid these peak intensity variations it is necessary to distribute the analyte as uniformly as possible within the non-absorbing background matrix.

Concentration: One particularly important advantage of diffuse reflectance spectroscopy, especially in comparison to transmittance measurement, is its extremely broad sample-analyzing range. While it is theoretically possible to acquire usable diffuse reflectance spectra on samples of wide-ranging concentrations, practical considerations often complicate the analysis process. With high concentration samples, especially those with a high refractive index, one can expect a dramatic increase in the specular contribution to the spectral data. As a result, some sample data may be un-interpretable without adequate sample dilution. Even when samples can be measured satisfactorily at high concentrations, it is advisable to grind the sample to a very uniform and fine particle size to minimize both specular reflectance and sample scattering effects, which adversely affect quantitative precision.

From the preceding paragraphs one can say that in reality, colour is in the eye of the observer, rather than in the "coloured" object. The property of an object that gives it a characteristic colour is its light-absorptive capacity. Three items (light source, object and observer) therefore are necessary for visual perception of colour and the instrument quantifies the human colour perception in the visual observing situation and we measure them in different units, scale or specification.

## 2.2 Colour Scales

There are three characteristics of light by which a colour may be specified: hue, saturation, and brightness. Hue is an attribute associated with the dominant wavelength in a mixture of light waves, i.e., it represents the dominant colour as perceived by an observer. Saturation refers to relative purity or the amount of white light mixed with a hue. Brightness is a subjective term, which embodies the chromatic notion of intensity. Hue and saturation taken together are called chromaticity. Therefore, a colour may be characterized by brightness and chromaticity. There are numerous colour scales, one may even develop their own scale for uniformity in comparison of their subsequent products. The basic colours however are only three: red, green and blue, and other colours are derived by mixing these three. The light reflected off of the object passes through a red, green and blue glass filter to simulate the standard observer functions for a particular illuminant. A photodetector beyond each filter then detects the amount of light passing through each filter and these signals are displayed as $X$, $Y$, and $Z$ values. The specifications of basic standards used in colourimetry however are based on definitions of The Commision de International de l'Eclairage (CIE) by general consent almost in all countries. Some industries however are also using Munsell System and atlas for their products.

### *2.2.1 CIE System*

The Commission Internationale de l'Eclairage (CIE) defined a system of describing the colour of an object based on three primary stimuli: red (700 nm), green (546.1 nm), and blue (435.8 nm). Because of the structure of the human eye, all

colours appear as different combinations of these. The amounts of red, green, and blue needed to form any given colour are called the' 'tristimulus" values, *X*, *Y*, and *Z*, respectively. Using the *X*, *Y*, and *Z* values, a colour is represented by a set of chromaticity coordinates or trichromatic coefficients, *x*, *y*, and *z*, as defined below:

$$x = \frac{X}{X+Y+Z} \quad y = \frac{Y}{X+Y+Z} \quad z = \frac{Z}{X+Y+Z} \tag{2.13}$$

It is obvious from the equations above that $x + y + z = 1$. The tristimulus values for any wavelength can be obtained from either standard tables or figures. A plot that represents all colours in *x* (red)-*y* (green) coordinates is known as a chromaticity diagram (Fig. 2.4).

To understand the chromaticity diagram, the locus is superimposed, with the reference horseshoe curve obtained from a standard monochromatic light. It can be seen from this figure that the chromaticity of unripe fruits falls near the center of the CIE diagram. The position marked "c" in this diagram represents colour, which is biochromatically achromatic or hueless. Oil palm actually appears reddish black when unripe and this agrees well with colourimeter since this equipment treats both pure white and black as hueless. As the fruit starts to ripen; the locus moves from the hueless zone to the reddish red zone and ends at a point bordering the reddish orange zone. It can be seen from this diagram that the difference in chromaticity between unripe and underripe is relatively small compared to the difference in chromaticity between optimally ripe and overripe, indicating that there is a small degree of change in colour at the early stage of ripening. The distance between unripe and overripe is 0.202 compared to slightly over 0.03 between unripe and under-ripe. Hence, distinguishing unripe from underripe samples or vice versa may be difficult chromatically.

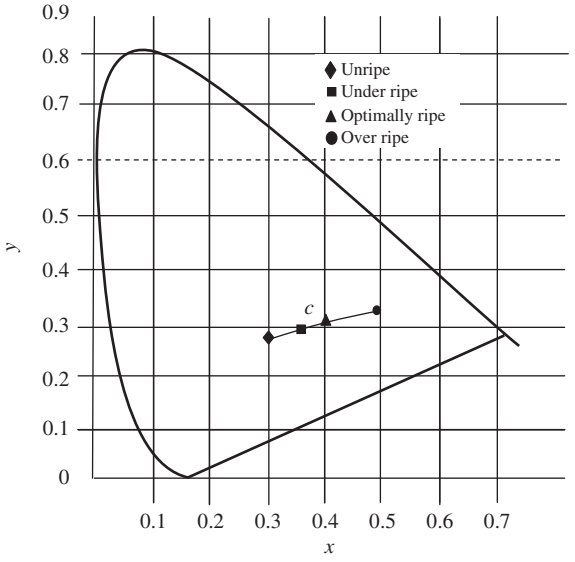


**Fig. 2.4** Schematic of chromaticity diagram showing the ripeness locus of oil palm and also the location of white in illuminant "c"

Sometimes, tristimulus systems of representation of colours are not easily understood by the users in terms of object colour. Other colour scales therefore were developed to relate better to how we perceive colour, simplify understanding, improve the communication of colour differences, and be more linear throughout colour space. This gave the birth of opponent colour theory, which states that the red, green and blue responses are re-mixed in opponent coders as they move up the optic nerve in human brain. Based on this theory a 3-dimensional rectangular *L*, *a*, *b*, colour space was evolved, in which at *L* (lightness) axis – 0 is black and 100 is white, *a* (red-green) axis – positive values are red; negative values are green and zero is neutral, and *b* (blue-yellow) – positive values are yellow; negative values are blue and zero is neutral (Fig. 2.5). All colours that can be visually perceived can be plotted in this *L*, *a*, *b*, rectangular colour space.

There are two popular *L*, *a*, *b* colour scales in use today – Hunter *L*, *a*, *b*, and CIE $L^*$, $a^*$, $b^*$. They are similar in organization, but will have different numerical values. Hunter *L*, *a*, *b* and CIE $L^*$, $a^*$, $b^*$ scales are both mathematically derived from *X*, *Y*, *Z* values (Table 2.2). Neither scale is visually uniform, Hunter scale is over expanded in blue region of colour space, while CIE scale is over expanded in yellow region. The current recommendation of CIE is to use $L^*$, $a^*$, $b^*$.

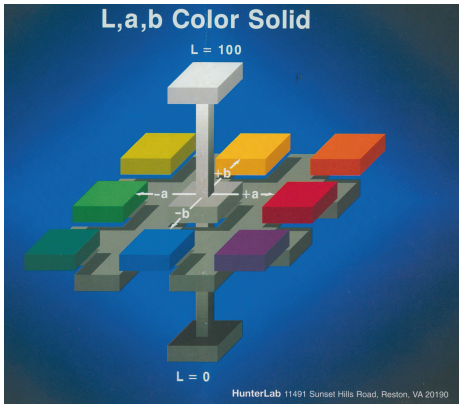


**Fig. 2.5** Hunter *Lab* colour space

**Table 2.2** Formulae for computation of *L*, *a*, *b*, and $L^*$, $a^*$, $b^*$ from *X*, *Y*, *Z* values

| Hunter *L*, *a*, *b* | CIE $L^*$, $a^*$, $b^*$ |
|---|---|
| $L = 100\sqrt{\frac{Y}{Y_n}}$ | $L^* = 116f\left(\frac{Y}{Y_n}\right) - 16$ |
| $a = K_a\left(\frac{X/X_n - Y/Y_n}{\sqrt{Y/Y_n}}\right)$ | $a^* = 500\left[f\left(X/X_n\right) - f\left(Y/Y_n\right)\right]$ |
| $b = K_b\left(\frac{Y/Y_n - Z/Z_n}{\sqrt{Y/Y_n}}\right)$ | $b^* = 200\left[f\left(Y/Y_n\right) - f\left(Z/Z_n\right)\right]$ |

Where, $Y_n$ is the $Y$ tristimulus value of a specified white object. For surface-colour applications, the specified white object is usually (though not always) a hypothetical material with unit reflectance and which follows Lambert's law. The resulting $L$ will be scaled between 0 (black) and 100 (white); roughly ten times the Munsell value. $K_a$ is a coefficient which depends upon the illuminant (for $D_{65}$, which will be told in latter part of the chapter, $K_a$ is 172.30; see approximate formula below) and $X_n$ is the $X$ tristimulus value of the specified white object. $K_b$ is a coefficient which depends upon the illuminant (for $_{D65}$, $K_b$ is 67.20; see approximate formula below) and $Z_n$ is the $Z$ tristimulus value of the specified white object, subscript $n$ suggests normalized values of $X$, $Y$, $Z$, and

$$f(t) = \begin{cases} t^{1/3} & t > (6/29)^3 \\ \frac{1}{3}\left(\frac{29}{6}\right)^2 t + \frac{4}{29} & otherwise \end{cases} \tag{2.14}$$

The division of the $f(t)$ function into two domains was done to prevent an infinite slope at $t = 0$. $f(t)$ was assumed to be linear below some $t = t_0$, and was assumed to match the $t^{1/3}$ part of the function at $t_0$ in both value and slope. In other words:

| | | | |
|---|---|---|---|
| $t_0^{1/3}$ | = | $at_0 + b$ | (match in value) |
| $1/3t_0^{2/3}$ | = | $a$ | (match in slope) |

The value of $b$ was chosen to be 16/116. The above two equations can be solved for $a$ and $t_0$:

$a = 1/(3\delta^2) = 7.787037\ldots$
$t_0 = \delta^3 = 0.008856\ldots$

where $\delta = 6/29$. Note that the slope at the join is $b = 16/116 = 2\delta/3$

$$K_a \approx \frac{175}{198.04}(X_n + Y_n)$$

$$K_b \approx \frac{70}{218.11}(Y_n + Z_n)$$

### 2.2.2 Munsell System and Atlas

The Munsell colour system (Fig. 2.6) divides hue into 100 equal divisions around a colour circle. This is similar in approach to the Newton colour circle except that the circle is distorted by assigning a unit of radial distance to each perceptible difference in saturation (called units of chroma). Since there are more perceptible differences

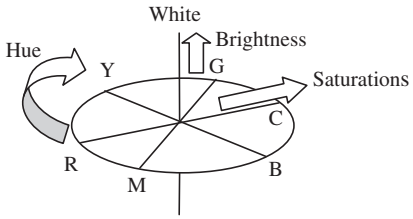


**Hue:** 100 quality spaced hues around circle
**Saturation:** units of "chroma" starting at 0 on the center line and increasing to values of 10 to 18 depending upon the hue. Some hues have more distinguishable levels of saturation.
**Brightness:** value from 0 for black to 10 for white

**Fig. 2.6** Schematic of Munsell colour system

for some hues, the figure will bulge outward to 18 for some hues compared to only 10 for others. Perpendicular to the plane formed by hue and saturation is the brightness scale divided into a scale of "value" from zero (black) to 10 (white). A point in the colour space so defined is specified by hue, value, and chroma in the form *H*, *V* and *C*. The Munsell colour-system is therefore a way of precisely specifying colours and showing the relationships among them. Every colour has three qualities or attributes: hue, value, and chroma. A set of numerical scales with visually uniform steps for each of these attributes has been established. The Munsell Book of Colour displays a collection of coloured chips arranged according to these scales. Each chip is identified numerically using these scales. Comparing it to the chips under proper illumination and viewing conditions can identify the colour of any surface. The colour is then identified by its hue, value, and chroma. These attributes are given the symbols *H, V*, and *C* and are written in a form *H V/C*, which is called the Munsell notations. Using Munsell notations, each colour has a logical relationship to all other colours. This opens up endless creative possibilities in colour choices, as well as the ability to communicate those colour choices precisely. The Munsell system is the colour order system most widely quoted in food industry literature. Food products for which the US Department of Agriculture (USDA) recommends matching Munsell discs to be used include dairy products such as milk and cheese, egg yolks, beef, several fruits, vegetables, and fruit juices.

Other colour atlases and charts are available for use in the food industry, such as the Natural Colour System and Atlas, Royal Horticultural Society Charts, etc. These atlases and charts are used for comparison of a product colour with that of a standard colour diagram, which is also commonly practiced in the food industry. The evaluation of potato chip colour is a very good example.

Other colour scales, such as the *RGB*, *CMY*, *HSI*, *HSV*, *HLS* etc. also exist, but are very similar to the CIE system. *RGB* system is generally used in analysis of colour of an image, while others are now not in much use for measurement of colour of food items, however have been dealt in detail in Chap. 3.

### *2.2.3 Transformation of Colour Values from One System to Others*

There are, as we have discussed above, various colour scales. These scales can be transformed from one to other forms, through simple trigonometric or mathematical

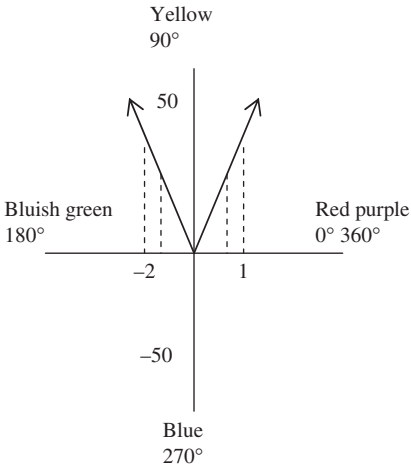


**Fig. 2.7** Representation of peel hue affected by heat treatments of grape fruits. *CIE LAB* $a^*$ and $b^*$ values are plotted on horizontal and vertical axes respectively

functions (Eqs. 2.15, 2.16 and 2.17). A colour wheel subtends 360°, with red-purple traditionally placed at the far right (or at an angle of 0°), yellow, bluish-green, and blue follow counter clockwise at 90, 180, 270°, respectively (Fig. 2.7).

$$L = L^* \tag{2.15}$$

$$h^0 = \tan^{-1} \frac{\mathrm{b}^*}{\mathrm{a}^*} \tag{2.16}$$

$$C^* = \sqrt{\left(a^{*2} + b^{*2}\right)} \tag{2.17}$$

Arctangent, however, assumes positive values in the first and third and negative values in the second and fourth quadrants. For a useful interpretation, $h^\circ$ should remain positive between 0 and 360° of the colour shed.

Figure 2.8 shows the variation of CIE*Lab* values calculated from the oil palm image. It can be seen that both hue and chroma increase in curvilinear fashion with ripeness. The small hue and chroma values for unripe class (approximately 7.6° and 2.62, respectively) pushed the psychometric point nearer to the origin or the achromatic zone of colour. These values increased to approximately 48° in hue and 72.1 in chroma for overripe case. This location is equivalent to reddish orange colour on CIE*Lab* space. Hence, the hue-moves further away from the origin and in the upward direction as the oil palm ripens. These observations are consistent with human vision and match strongly with the trend of the ripeness locus shown in Fig. 2.4. Thus hue provides a much better discrimination compared to either *RGB* or CIE*xy* values when specifying colours of food materials. Because of this reason usually hue is chosen for colour inspection by machine.

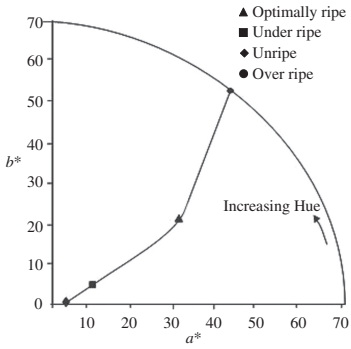


**Fig. 2.8** Schematic of colourimetric plot of oil palm showing the change in hue and chroma during ripening

Unlike colourimeter, the calculation of hue using machine vision system is mathematically involved since it requires colour conversion from *RGB* to *HSl* (Hue, Saturation and Intensity) space. One way of achieving this is by firstly *I* establishing a new coordinate system, *YIQ*. The relationship between the two coordinate systems is:

$$\begin{bmatrix} Y \\ I \\ Q \end{bmatrix} = \begin{bmatrix} 0.30 & 0.59 & 0.11 \\ 0.60 & -0.28 & -0.32 \\ 0.21 & -00.52 & 0.31 \end{bmatrix} \begin{bmatrix} R \\ G \\ B \end{bmatrix} \tag{2.18}$$

Secondly, $h$ is the rotational angle around the $Q$, $I$ plane and therefore can be written as:

$$h^o = \tan^{-1}\left[\frac{I}{Q}\right] \tag{2.19}$$

Equations (2.18) and (2.19) are theoretically valid and they can be found in almost any textbook on colour and image processing. For practical reasons, $h°$ was calculated according to the Munsell's colour system, which is given by:

$$h^o = \left\{360^o - \cos^{-1}\left(\frac{-0.5\left[(R-G)+(R-B)\right]}{\sqrt{(R-G)^2+(R-B)(G-B)}}\right)\right\} \times \frac{255}{360} \; if \; B \geq G \tag{2.20}$$

or

$$h^o = \left\{\cos^{-1}\left(\frac{-0.5\left[(R-G)+(R-B)\right]}{\sqrt{(R-G)^2+(R-B)(G-B)}}\right)\right\} \times \frac{255}{360} \; if \; B < G \tag{2.21}$$

The above equation transforms *RGB* information from three-dimensional space to one-dimensional $h°$ space. In order to speed-up analysis only $h°$ values may be processed. The hue values shown in this figure are normalized to 255 for the 8-bit

machine vision system. A different approach is needed to solve this type of problem. The method investigated for this application was to treat hue distributions as features and apply multivariate discriminate technique to establish classification as discussed in Chap. 6.

#### 2.2.3.1 Example of Transformation of CIE/Hunter *L a b* Values to Chroma (*C*) and Hue (*h*°)

Assume a practical data given in Table 2.3 for analysis of grapefruit colour after three heat treatments for quarantine control

Following subprogram may be used to compute the $h°$ and $C$ for above data

```
Data colour
READ (* ,* ) L, a, b
C=SQRT((a* b)+(b* b))
THETA=(ATAN(b/a)/6.2832)* 360
IF a>0 AND b>=0 THEN h = THETA
IF a<0 AND b>=0 THEN h=180+THETA
IF a<0 AND b<0 THEN h=180+THETA
IF a>0 AND b<0 THEN h=360+THETA
WRITE (* ,* ) a, b, THETA, h
STOP
END
```

**Table 2.3** Conversion of grapefruit *L a b* values to hue and chroma values

| | Colour characteristics | | | | |
|---|---|---|---|---|---|
| Treatment | *L* | *a* | *b* | *C* | *h*° |
| 1 | 76.6 | –2.0 | 56.0 | 56.0 | 92.0 |
| 2 | 74.4 | 2.0 | 56.0 | 56.0 | 88.0 |
| 3 | 63.0 | 1.2 | 34.0 | 34.0 | 88 |

## 2.3 Colour Measurement

It is clear by now that to see colour three things (light source, object and the observer) are needed. Similarly to measure colour three items are essential: light source, specimen object and a spectrometer (colourimeter). When we have spectrometer or colourimeter the user first goes through the operational manual of the instrument thoroughly to see the suitability for their specimen object, i.e. sample. Once suitability is judged then colour scale, illuminant and observer types, if options are available in the instrument, are selected. CIE standard illuminants are $D_{50}$, $D_{55}$, $D_{65}$.

### 2.3.1 CIE Standard Illuminants

$D_{65}$ is a commonly used standard illuminant defined by the CIE. It is part of the D series of illuminants that try to portray standard illumination conditions at open air in different parts of the world. The subscript 65 probably is used to indicate the correlated colour temperature of 6,500 K at which it is standardized. $D_{65}$ corresponds roughly to a mid-day sun in Western Europe/Northern Europe, hence it is also called a daylight illuminant. As any standard illuminant is represented as a table of averaged spectrophotometric data, any light source which statistically has the same relative spectral power distribution can be considered a $D_{65}$ light source. There are no actual $D_{65}$ light sources, only simulators. The quality of a simulator can be assessed with the CIE Metamerism index discussed elsewhere. $D_{65}$ should be used in all colourimetric calculations requiring representative daylight, unless there are specific reasons for using a different illuminant. Variations in the relative spectral power distribution of daylight are known to occur, particularly in the ultraviolet spectral region, as a function of season, time of day, and geographic location.

### 2.3.2 CIE Standard Observers

CIE has standardized the observer angle of field of view. Originally this was taken to be the chromatic response of the average human viewing through a 2° angle, due to the belief that the colour-sensitive cones resided within a 2° arc of the fovea of human eye. Thus the CIE *1931 Standard Observer* is also known as the CIE *1931 2° Standard Observer*. Latter it was experimentally decided that cones were spread beyond the fovea. The experiments were repeated in 1964 resulting in 1964, 10° standard observer. Of the two sets of observer function, the 10° standard observer is recommended for better correlation with average visual assessment made with large fields of view that is typical in most commercial application.

### 2.3.3 Instrument Geometry

A third important aspect for selection before actual experimentation is instrument geometry. The geometry of an instrument defines the arrangement of light source, sample plane, and detector. There are two general categories of instrument geometries, directional (45°/0° or 0°/45°) and diffuse (sphere). Directional geometry typically has illumination at 45° angle and a measurement angle of 0° (meaning from top of the object or from direction perpendicular to the sample). This is called 45°/0° geometry. 0°/45° geometry has illumination at 0° and measurement at 45°. Both exclude the specular reflection in the measurement. This provides measurements that correspond to visual changes in appearance of the sample due to both changes in pigment colour and surface gloss or texture. 0°/45° instrument geometry as I think is the best for the quality determination and monitoring applications.

The fourth and the last consideration for colour measurement is the preparation and presentation of the prepared samples as discussed below.

## 2.4 Sample Preparation and Presentation

Availability of wide range of techniques for measurement of quality parameters, necessitates to know the suitability of characteristics of samples, i.e. whether it is liquid, solid, paste, semisolid, transparent, opaque or translucent etc for a particular technique to be employed. Complete history of the source of sample and a careful attention to proper instrument operation and consistent sample handling is required particularly for colour measurement.

### *2.4.1 Preparing Samples for Measurement*

During sample measurement it is important to select them appropriately, using an established method of sampling, and handling all samples in a consistent manner.

(a) Selecting samples
Sample representative of the entire batch should be selected for measurement. One should always try to collect as number of varied materials as possible from different sources whose colour is to be measured and

1. Choose samples that are truly representative of the materials collected from various sources,
2. prepare samples in exactly the same manner each time they are measured. Follow standard method, if they exist such as ASTM, BIS etc, and
3. present the sample to the instrument in a standard, repeatable manner. Results obtained depend on the condition of the sample and their presentation. For established procedure, make a checklist so that laboratory personnel may simply check each step. The checklist will also help in training of new workers.

The sample must also be representative of attributes that are of interest. If samples are non-representative of the batch or are spoiled, damaged, or irregular, then the sample may be biased. While choosing a sample, select in random fashion and examine the sample to avoid biased results. If sampling procedures are adequate, a different sample selected from the same batch should result in comparable measured values.

(b) Sample handling and presentation methods
If method of measurement is established so that same procedure is used each time for specific samples or types of samples, results may be validated for comparison purposes. This also insures repeatability of results when measuring the same sample.

There are a variety of techniques that can be used in handling various forms of objects and materials so that the most valid and repeatable measurement of their appearance results. Consideration must be given to the conditions for sample preparation that are dependent upon the type of measurement to be made. For example, when measuring the colour of sample that might spill into the viewing aperture, one should hold the surface flat by using a cover glass taped over the aperture window. Other materials being measured for colour may be chopped up and placed in a glass specimen cell or made into paste and applied to a glass plate. Sheets and films should be flattened by tension or by a vacuum, if necessary.

(c) Directional samples

Averaging several measurements with rotation of the sample between readings can minimize directionality. Examination of the standard deviation displayed with the average function can guide in selecting the appropriate number of readings to average.

(d) Non-opaque samples

Non-opaque samples must have a consistent backing. A white un-calibrated tile is recommended. If the sample is such that it can be folded to give multiple layers, such as fruit leather, the number of layers for each sample should be noted.

(e) Translucent samples

Light trapped in a translucent sample can distort the colour. The thickness of the sample presented should be chosen to maximize the haze or colour difference.

(f) Granular, powdery and liquid samples

These foods in required quantity may be taken into a petri dish of known composition and characteristics and covered by other complete transparent and flat petty dish of known properties. Thickness or depth of the sample should be so maintained that it presents an opaque mass. Colour readings may be taken keeping the flat portion of nosecone of the colourimeter on the surface of the top petty dish ensuring that light thrown by the instrument neither goes out of the nosecone nor passes through the sample. Part of the light is absorbed by the sample and remaining portion (reflected from the sample) again comes back to the nosecone of the instrument for measurement and interpretation. If samples cannot be prepared to make it opaque (in case of transparent liquid sample) instruments such as tintometer, photospectrometer etc are better to use.

## 2.5 Error in Colour Measurement

Every measurement has a chance of error, and colour measurement is not an exception. It has possibly two source of error: first may be due to instrument and second, error in measurement. Instrumental errors are based on instrument you are using. They are enumerated below:

- Errors in absolute scales of diffuse reflectance and 0/45 radiance factor.
- Errors due to differing properties of white reference standards.

- Non-linearity of the photodetector.
- Incorrect zero level.
- Wavelength scale error.
- Specular beam exclusion error.
- Specular beam weighting error.
- Errors due to non-uniformity of collection of integrating spheres.
- Polarisation errors in the 0/45 geometry.
- Differences in methods for calculating colour data from spectral data.
- Errors due to thermochromism in samples.
- Errors due to the dependence of spectral resolution on band width, scan speed and integration time.
- Geometry difference between illumination and collection optics within the specified limits.

At present, there is no method for quantifying the effects of geometry differences (last item) and applying corrections. The method used to minimise error due to non-uniformity of collection by integrating spheres, which is to measure matt samples against matt masters and glossy samples against glossy masters, has not proved very effective. Integrating sphere errors are due to the fact that the integrating sphere is not an ideal sphere but a hemispherical sphere. There are also some baffles inside the sphere which prevent straight light from striking the detector.

Possibilities of error during measurement are due to following reasons:

(i) Nosecone of the instrument and surface of sample is not having good agreement and thus leakage of light
(ii) Samples are non-uniform, translucent or transparent and cause leakage or escape of light during measurement.
(iii) Improper alignment of colourimeter with sample surface
(iv) Surface of reference plate is not properly maintained and does not give reference values supplied by the manufacturer
(v) Error due to incorrect type of sample for the instrument

It is now clear that there are significant undetermined errors. Instrumental error, if any, should be checked and minimized with the help of manufacturer while error due to measurement will be minimized with due care by the users. Accounted errors should be measured and analysed properly for reporting.

## 2.6 Colour Analyses and Modeling

Colour values are generally analysed to see the colour difference in comparison with the standard specimen, to see the trends of changes with storage or processing conditions and are modeled sometimes to correlate with the specific attributes of the products. Colour difference nowadays can directly be obtained using most of the colourimeter, while for correlating colour values with any attributes; regression analyses are performed.

### 2.6.1 Colour Difference

Colour difference is always calculated as colour values of sample minus that of standard specimen. If $\Delta L^*$ is positive than sample is lighter than the standard. If negative, it would be darker than the standard. If $\Delta a^*$ is positive, the sample is more red or less green than the standard. If it is negative, it would be greener or less red. Similarly if $\Delta b^*$ is positive, the sample is more yellow or less blue than the standard. If negative, it would be bluer or less yellow. Now question arises what should be the acceptable colour difference? The simple answer is the minimum perceptible colour. What should be the acceptable tolerance? In theory the total colour difference of 1.0 is supposed to be indistinguishable unless samples are adjacent to one another. Colour difference can be computed using the following formulas.

$$\begin{aligned} \Delta L^* &= L_2^* - L_1^*, \Delta a^* = a_2^* - a_1^*, \Delta b^* = b_2^* - b_1^* \quad \text{and} \\ \Delta E_{ab}^* &= \sqrt{\left(L_2^* - L_1^*\right)^2 + \left(a_2^* - a_1^*\right)^2 + \left(b_2^* - b_1^*\right)^2} \end{aligned} \tag{2.22}$$

Where subscript 1 is for standard specimen and 2 is for sample and $E_a{}^*{}_b$ is total colour difference. It is intended to be a single number metric to have decision to pass or fail the sample. $\Delta E$ itself is not always reliable, because it is non uniform in colour space. It is therefore better, if can be, to set the tolerance limit for individual colour values.

### 2.6.2 Colour Modeling

Modeling is a very useful tool for (relatively) quickly and inexpensively ascertaining the effect of any system and parameters on the outcome of a process or effect of parameters. The benefit of modeling is to minimize the number of experiments that need to be conducted to know the effect of individual parameter. Models broadly can be divided into two types: theoretical mathematical model and empirical or regression model. The first one becomes more accurate and generalized while the second one is developed for a particular process or products and its accuracy depend on the accuracy in experimental values used in development and regression coefficient of determination of such models. In colour modeling majority of scientists have used the second type of modeling. Any modeling process can roughly be divided into five phases.

- First step is problem identification, i.e., what you want to predict using the developed model
- The second step consists of constructing a mathematical model for the corresponding problems. This could be in the form of differential or algebraic equations.
- In third phase the mathematical model is converted to numerical model by doing some approximation for easy solution.

- The fourth phase is the solution of the numerical model. It is generally not required if modeling is empirical or regression equation.
- Fifth and the final phase is validation of solution or predictions done by the model in real situations

## 2.7 Practical Applications

Numerous works on colour analyses and modeling of colour values of food materials are reported in literature, majority of them however are based on colour values extracted from the specimen's images. Some of them are covered in the Chap. 3. This chapter is limited to the most recent work on analyses of colour values acquired in terms of CIE colour scale and usually using a colourimeter.

### *2.7.1 Vegetables*

The green colour of vegetables changes considerably during heat treatments like blanching and has been modeled using simplified kinetic mechanisms (Tijskens et al. 2001). Validation of model indicated that the formation and degradation of visible colour in vegetables is governed by processes related to the colouring compounds $\check{Z}$ like chlorophyll and chlorophilides, irrespective of the vegetables under study. This study helped in understanding of chlorophyll degradation and gave generalized information for any vegetable. But in another study (Martins and Silva 2002) on chlorophyll degradation of frozen green beans using Hunter colour values *a, b* and total colour difference in first order and reversible first order models revealed that colour is a more important parameter to asses frozen greens visual quality however chlorophyll content is not a good colour index for the same. Trends of chromatic changes of broccoli under modified atmosphere packaging (MAP) at 20°C in perforated and unsealed polypropylene film packages for a storage period of 10 days indicated using $L^*C^*h^*$ colour space diagram that the modified atmosphere (6.1% $O_2$ and 9% $CO_2$) generated inside the perforated film packages having 4 macro-holes was the most suitable in maintaining the chromatic quality of the broccoli heads (Rai et al. 2009). Postharvest life of tomatoes is limited by colour as one of the important parameters. One colour model correlates the colour level and biological age at harvest (Schouten et al. 2007). Data were analysed using non-linear regression analysis and found that biological age of tomato can well be predicted at farmers' level and can save lot of postharvest losses of tomato especially during the glut. Interestingly they also found very good correlation among the colour values and firmness of tomato.

### *2.7.2 Fruits*

The different combinations of *L*, *a* and *b* colour values have been fitted in different form of linear models (Table 2.4) and regressed using multiple linear regression,

**Table 2.4** Generalized forms of maturity index ($I_m$) models tested in terms of colour values ($L$, $a$, $b$)

| Model no. | Variables | Models* |
|---|---|---|
| 1 | $a$, $b$, $L$ | $I_m = C_1 + C_2a + C_3b + C_4L$ |
| 2 | $a$, $b$ | $I_m = C_1 + C_2a + C_3b$ |
| 3 | $a$, $b$, $a \times b$ | $I_m = C_1 + C_2a + C_3b + C_4ab$ |
| 4 | $a$, $b$, $a^2$, $b^2$, $a \times b$ | $I_m = C_1 + C_2a + C_3b + C_4ab + C_5a^2 + C_6b^2$ |
| 5 | $a^2$, $b^2$ | $I_m = C_1 + C_2a^2 + C_3b^2$ |
| 6 | $b$, $a \times b$ | $I_m = C_1 + C_2b + C_3ab$ |

*$C_1$, $C_2$, $C_3$ are models' constants.

partial least squares and principal component regressions to maturity index of mango (Jha et al. 2007, 2009). Precision of prediction using models having the parameters of $a$, $b$ and their product ($a \times b$) was verified by sensory evaluation of 55 ripe mangoes and was found that the fruits predicted to be mature could ripe with high-satisfied taste while the ones predicted to be immature or over mature were mostly rejected by the panels (Jha et al. 2007). Latter a colour chart for Dusheri cultivar of mango was developed to read the maturity or ripeness level after taking the values of $a$ and $b$ of mango in tree using a handheld colourimeter (Fig. 2.9). It is evident from the study that internal quality parameters of mango (Jha et al. 2006b) are correlated with the colour values and can be predicted satisfactorily. Similarly a freshness index/over all quality index for five cultivars of apple was developed in which colour values are important factors (Jha 2007, Jha et al. 2010, 2010a). The relationship between colour parameters and anthocyanins of four sweet cherry cultivars using $L^*$, $a^*$, $b^*$, chroma and hue angle parameters (Berta et al. 2007) indicated that chromatic functions of chroma and hue correlate closely with the evolution

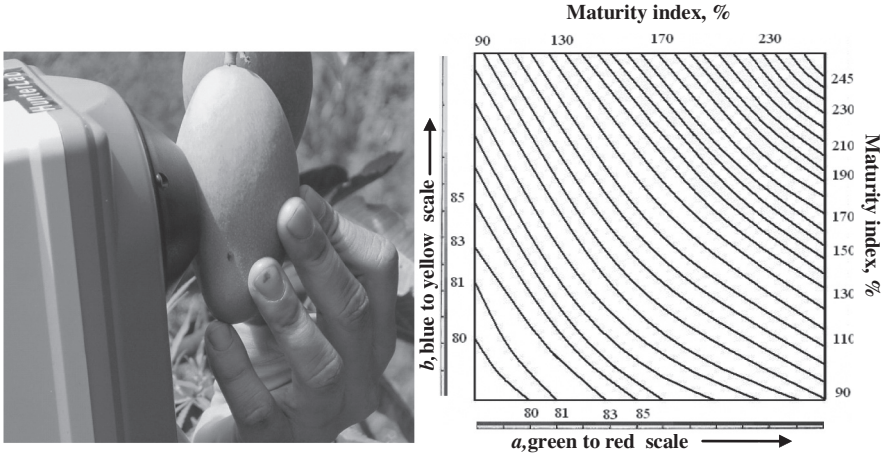


**Fig. 2.9** Measurement of maturity and ripeness of mango in tree

of colour and anthocyanins levels during storage of sweet cherries and that colour measurements can be used to monitor pigment evolution and anthocyanin contents of cherries.

Tiwari et al. (2008) used response surface methodology to develop the empirical model to study the effect of ozonation on orange juice colour degradation and found that predicted colour values obtained using model equations were in good agreement with the experimental values. Mathematical equations using *L*, *a*, and *b* developed by Atilla (2007) for predicting the optimum roasting degree of hazelnut and reported that *a* and *L* values gave high $r^2$ and obtained three-dimensional nonlinear equations to determine the optimum roasting degree based on time and temperature.

The above paragraphs indicate that significant attempts have been made to model colour values or combination thereof for prediction of various surface as well as internal quality parameters of various fruits and vegetables. Very limited work however on modeling of colour values of other foods such as food grain, oilseeds etc. are reported for prediction of their quality parameters. The coefficient of determination of these models may not be sometimes as high as it is expected. In such cases one may try to obtain the complete spectra of specimen instead of individual colour values (*L*, *a*, *b* etc.) in the visible range of wavelength (400–700 nm) and develop models using the absorption or reflectance data (Jha et al. 2006a, 2005).

## References

Atilla S (2007) The use of 3d-nonlinear regression analysis in mathematical modeling of colour change in roasted hazelnuts. J Food Eng 78:1361–1370

Berta GA, Ana PS, Jose MP et al (2007) Effect of ripeness and postharvest storage on the evolution of colour and anthocyanins in cherries (*Prunus avium* L.). Food Chem 103:976–984

Jha SN (2007) Final report (RPF III) of research project on development of nondestructive methods for quality evaluation of apple. Central Institute of Post-Harvest Engineering and Technology, Ludhiana, India

Jha SN, Chopra S, Kingsly ARP (2005) Determination of sweetness of intact mango using visual spectral analysis. Biosyst Eng 91(2):157–161

Jha SN, Chopra S, Kingsly ARP (2007) Modeling of color values for nondestructive evaluation of maturity of mango. J Food Eng 78:22–26

Jha SN, Chopra S, Kingsly ARP (2009) On-farm nondestructive determination of maturity of intact mango fruit. Indian Journal of Horticulture 66(3): 353–357

Jha SN, Kingsly ARP, Chopra S (2006a) Nondestructive determination of firmness and yellowness of mango during growth and storage using visual spectroscopy. Biosyst Eng 94(3):397–402

Jha SN, kingsly ARP, Chopra S (2006b) Physical and mechanical properties of mango during growth and storage for determination of maturity. J Food Eng 72(1):73–76

Jha SN, Rai DR, Gunasekaran S (2010) Visual spectroscopy and colour modeling for nondestructive evaluation of quality of apple. J of Agric Engineering – accepted

Jha SN, Rai DR, Sharma R (2010a) Physico-chemical quality parameters and overall quality index of apple during storage. J Food Sci and Technol – accepted

Martins RC, Silva CLM (2002) Modeling colour and chlorophyll losses of frozen green beans (*Phaseolus vulgaris* L.). Int J Refrig 25:966–974

Rai DR, Jha SN, Wanjari OD et al (2009) Chromatic changes in broccoli (*Brassica oleracea italica*) under modified atmospheres in perforated film packages. Food Sci Technol Int 15(4):387–395

Schouten RE, Huijbeb TPM, Tijskens LMM et al (2007) Modeling quality attributes of truss tomatoes: linking colour and firmness maturity. Postharvest Biol Technol 45:298–306

Tijskens LMM, Schijvens EPHM, Biekman ESA (2001) Modeling the change in colour of broccoli and green beans during blanching. Innov Food Sci Emerg Technol 2:303–313

Tiwari BK, Muthukumarappan K, Donnell CPO et al (2008) Modeling colour degradation of orange juice by ozone treatment using response surface methodology. J Food Eng 88(4): 553–560

http://www.springer.com/978-3-642-15795-0

Nondestructive Evaluation of Food Quality
Theory and Practice
Jha, S.N. (Ed.)
2010, XI, 288 p., Hardcover
ISBN: 978-3-642-15795-0